

5-1-2020

## Targeting EGFR Overexpression at the Surface of Colorectal Cancer Cells by Exploiting Amidated BODIPY-Peptide Conjugates

Tyrslai M. Williams  
*Louisiana State University*

Zehua Zhou  
*Louisiana State University*

Sitanshu S. Singh  
*University of Louisiana at Monroe*

Martha Sibrian-Vazquez  
*Louisiana State University*

Seetharama D. Jois  
*University of Louisiana at Monroe*

*See next page for additional authors*

Follow this and additional works at: [https://digitalcommons.lsu.edu/chemistry\\_pubs](https://digitalcommons.lsu.edu/chemistry_pubs)

---

### Recommended Citation

Williams, T., Zhou, Z., Singh, S., Sibrian-Vazquez, M., Jois, S., & Henriques Vicente, M. (2020). Targeting EGFR Overexpression at the Surface of Colorectal Cancer Cells by Exploiting Amidated BODIPY-Peptide Conjugates. *Photochemistry and Photobiology*, 96 (3), 581-595. <https://doi.org/10.1111/php.13234>

This Article is brought to you for free and open access by the Department of Chemistry at LSU Digital Commons. It has been accepted for inclusion in Faculty Publications by an authorized administrator of LSU Digital Commons. For more information, please contact [ir@lsu.edu](mailto:ir@lsu.edu).

---

**Authors**

Tyrslai M. Williams, Zehua Zhou, Sitanshu S. Singh, Martha Sibrian-Vazquez, Seetharama D. Jois, and Maria da Graça Henriques Vicente

MR. SITANSHU SINGH (Orcid ID : 0000-0003-3141-0224)

DR. MARIA DA GRACA H. VICENTE (Orcid ID : 0000-0002-4429-7868)

Article type : Special Issue Research Article

**Special Issue Research Article**  
**Targeting EGFR Overexpression at the Surface of Colorectal Cancer Cells by**  
**Exploiting Amidated BODIPY-Peptide Conjugates<sup>†</sup>**

*Tyrslai M. Williams<sup>1</sup>, Zehua Zhou<sup>1</sup>, Sitanshu Singh<sup>2</sup>, Martha Sibrian-Vazquez<sup>1</sup>, Seetharama D. Jois<sup>2\*</sup> and  
M. Graça H. Vicente<sup>1\*</sup>*

<sup>1</sup>*Department of Chemistry, Louisiana State University, Baton Rouge LA, 70803, United States*

<sup>2</sup>*School of Basic Pharmaceutical and Toxicological Sciences, College of Pharmacy, University of  
Louisiana at Monroe, Monroe LA 71201, United States*

\*CORRESPONDING AUTHOR'S EMAIL: [vicente@lsu.edu](mailto:vicente@lsu.edu) (Maria de Graça Vicente)

<sup>†</sup>This article is part of a Special Issue dedicated to Dr. Thomas Dougherty.

This is the author manuscript accepted for publication and has undergone full peer review but has not been through the copyediting, typesetting, pagination and proofreading process, which may lead to differences between this version and the [Version of Record](#). Please cite this article as [doi: 10.1111/PHP.13234](https://doi.org/10.1111/PHP.13234)

This article is protected by copyright. All rights reserved

## ABSTRACT

Three BODIPY-peptide conjugates designed to target the epidermal growth factor receptor (EGFR) at the extracellular domain were synthesized and their specificity for binding to EGFR was investigated. Peptide sequences containing seven amino acids, GLARLLT (**2**) and KLARLLT (**3**), and 13 amino acids, GYHWYGYTPQNVI (**4**), were conjugated to carboxyl BODIPY dye (**1**) by amide bond formation in up to 73% yields. The BODIPY-peptide conjugates and their “parent” peptides were determined to bind to EGFR experimentally using SPR analysis, and were further investigated using computational methods (AUTODOCK). Results of SPR, competitive binding, and docking studies propose that conjugate **6** including the GYHWYGYTPQNVI sequence binds to EGFR more effectively than conjugates **5** and **7**, bearing the smaller peptide sequences. Findings in human carcinoma HEP2 cells overexpressing EGFR showed nontoxic behavior in the presence of activated light (1.5 J/cm<sup>2</sup>) and in the absence of light for all BODIPYs. Furthermore, conjugate **6** showed about 5-fold higher accumulation within HEP2 cells compared with conjugates **5** and **7**, localizing preferentially in the cell ER and lysosomes. Our findings suggest that BODIPY-peptide conjugate **6** is a promising contrast agent for detection of colorectal cancer and potentially other EGFR over-expressing cancers.

## INTRODUCTION

Cancer is one of the most devastating ailments to cure in the world due to its genetic irregularity, effects, and indicators. Colorectal cancer (CRC), also known individually as colon, rectal, or bowel cancer, ranks as the third most common cancer diagnosed in both men and women when reviewed separately in the United States.<sup>1</sup> Current studies suggest that CRC age specificity is now escalating as previously seen with patients who were born around the 1890s.<sup>2</sup> Expected to cause nearly 51,020 fatalities in the year 2019, it is vital that science uncovers new methods for earlier detection. Several methods currently exist for detecting CRC such as fecal blood test and colonoscopy, however, these methods tend to have low sensitivity for detecting adenomas of less than 5 mm, typical of early stages of CRC.<sup>2</sup> Adenomas associated with CRC tend to lack outward patient symptoms making detection of CRC challenging.<sup>2</sup> Confocal Laser Endomicroscopy (CLE) has become an enhanced method of detecting CRC due to the high-resolution optical images obtained and the provided depth selectivity during ongoing endoscopic procedures.<sup>3</sup> Common contrast agents typically used with CLE, including cresyl violet blue, acrivlavin, and fluorescein, are not cancer cell-specific due to their untargeted nature.<sup>4</sup> To combat this

issue targeting the cell surface receptors, epidermal growth factor receptor (EGFR) offers a method for increased specificity. EGFR is a ligand-stimulated receptor that plays a crucial role in the regulation of cellular functions, comprising cell proliferation and survival.<sup>5-8</sup> Moreover, the single polypeptide backbone chain of EGFR has proven to be an integral piece in investigating effective treatments for cancers, such as CRC. About 98% of colon cancers have EGFR present and are adequately over-expressed on other small cancers including, but not limited to, non-small cell lung cancer (NSCLC), breast, head and neck (SCCHN), gastric colorectal, esophageal, prostate, bladder, renal, pancreatic, and ovarian cancers.<sup>9,10</sup> While the overexpression of EGFR is considered a mutation,<sup>11</sup> the alteration is attributed to the binding of EGFR to one of its endogenous ligands, EGF.<sup>12</sup> Several different practices have been advanced for targeting EGFR,<sup>6</sup> including FDA-approved anti-EGFR antibody cetuximab,<sup>13-15</sup> single-chain anti-EGFR ScFvEGFR,<sup>16</sup> anti-EGFR affibody,<sup>17,18</sup> accessible small peptides,<sup>9,10, 19-24</sup> and non-peptidic tyrosine kinase inhibitors.<sup>25</sup>

The detection of EGFR's significance to CRC and other cancers has resulted in the detection of peptide ligands, with high specificity for the EGF receptor. Among these ligands, those containing smaller sequences are particularly of interest for EGFR-targeting due to their adaptation and conjugation to a wide variety of molecules. Screen phase display libraries and computer-based design were used to identify two peptides LARLLT (designated "D4" or EGFR-L1) and YHWYGYTPQNVI (designated "GE11" or EGFR-L2).<sup>9,10</sup> Song and Li were able to prove especially efficient binding to the extracellular domain of EGFR overexpressed on the surface of cancer cells with these short peptide sequences. This binding has been established *in vitro* using various cell lines, such as SKBR-3 and BT-474 cells, and *in vivo* using A431 tumor-bearing nude mice.<sup>9,10, 19-23, 26,27</sup> Additionally, determination of successful binding of these peptides to EGFR protein extracellular domain has been detected via computational studies.<sup>9,10,23 27-29</sup> While EGFR-L1 binds near domain I, EGFR-L2 binds within the EGF binding pocket with strong binding affinity. However, the hydrophobic character of the EGFR-L2 sequence caused aqueous solubility issues when compared to the cationic EGFR-L1.<sup>23,28-31</sup>

4,4-Difluoro-4-bora-3a,4a-diaza-s-indacenes (BODIPYs) have been extremely useful as fluorescent labels due to their adaptability and solubility, as well as their exceptional photophysical properties.<sup>32</sup> BODIPYs maintain a highly spectroscopic tunable core structure that is stable under various conditions.<sup>32-36</sup> Developing efficient methods for conjugating BODIPY dyes to peptides requires that a clear position for attachment be present at each molecule. In peptide synthesis, the most evident attachment point is the exposed free amino group at the N-terminus of the sequence that can experience a variety of alterations, however, the most common method is amidation. The simplicity of formation for peptide synthesis is also attractive, however, the required counterpart, carboxyl-substituted BODIPY dyes

are often challenging. Carboxyl BODIPYs are not easily developed and are most often prepared via 2,6-<sup>37,38</sup> or 3,5-functionalizations<sup>39,40</sup> on the BODIPY core. Past synthetic approaches to achieve carboxyl BODIPY dyes involved protection/deprotection steps that caused potential issues<sup>41</sup> since the BODIPY core can be unstable under prolonged basic conditions.<sup>42-45</sup> Consequently, carboxylic BODIPYs with simpler and more expedient syntheses are significant for their practical applications. In 2009, a method for carboxylic BODIPY formation that bypassed the need for mixed pyrrole condensations was reported by Wang et al.<sup>46</sup> These efforts revealed a method to achieve the desired BODIPY core bearing a free carboxylic acid, using a one-pot, two-step reaction under relatively mild conditions, albeit in low to moderate yields, up to 25%. More recently Ksenofontova et al.<sup>47</sup> reported the spectral benefits of the conjugation of activated carboxyl BODIPYs to amino acids under standard peptide synthesis conditions (pH 11.0, 12 h at 2 °C).

In this work, we report an optimized higher yielding synthesis of carboxyl BODIPY dye **1** bearing a free carboxylic acid group, in a one-pot three-step reaction. The conjugation of this BODIPY to three different peptides, GLARLLT (**2**), KLARLLT (**3**), and GYHWYGYTPQNVI (**4**) afforded conjugates **5**, **6**, and **7** in yields up to 73% after purification by HPLC. SPR, competitive binding, and computational studies were performed and indicated both specific and non-specific binding to EGFR extracellular domain (ECD), while studies in the model human carcinoma (HEp2) cells showed low cytotoxicity for all conjugates.

## MATERIALS AND METHODS

**Synthesis.** Commercially available reagents were obtained from Sigma-Aldrich and VWR. Chemicals purchased were used without any additional purifications for the reactions and refinements. To monitor reactions, thin layer chromatography (TLC) was achieved with pre-coated silica gel plates (0.2 mm, 254 indicator, polyester backed, 60Å, Sorbent Technologies). Preparative TLC plates (60G, VWR) and silica gel (60Å, 230-400 mesh, Sorbent Technologies) were used for purification by preparative thin layer and flash column chromatography, respectively. <sup>1</sup>H NMR spectra was collected on a Bruker AV-400 liquid and <sup>13</sup>C NMR on a AV-500 spectrometer at 308K. All the chemical shifts ( $\delta$ ) are expressed in parts per million (ppm) in either CDCl<sub>3</sub> (7.27 ppm for <sup>1</sup>H NMR and 77.0 ppm for <sup>13</sup>C NMR) or DMSO (2.54 ppm for <sup>1</sup>H NMR), and coupling constants (*J*) are reported in Hz. Mass Spectra was obtained from the LSU Mass Spectrometry Facility using high-resolution mass spectra (HRMS) and MALDI (TOF) spectra on a 6210 ESI-TOF Mass Spectrometer (Agilent Technologies) under positive or negative mode. Additional separations were performed using Reverse-phase HPLC analysis on a Waters 2485 Quaternary Gradient Module, Waters Sample Injector, and 2489 UV/Visible Detector, which are controlled by Waters Empower 2 software. Purifications were carried out using an X-Bridge BEH300 Prep C18 (5  $\mu$ m, 10 x 250 mm) complete with an X-Bridge BEH300 Prep Guard cartridge at 300 Å (5  $\mu$ m, 10 x 10 mm) with a

flow rate of 4 mL/min flow rate and UV detection at 220 nm for peptides, and 499 nm for BODIPY conjugates. Fractions of the desired products with the expected mass and desired HPLC purity (> 95%) were combined and lyophilized.

**BODIPY 1.** In an oven-dried flask equipped with a stirrer, methyl magnesium chloride in 3M diethyl ether (0.237g, 1.98 mmol) was added to 2,4-dimethylpyrrole (0.171 g, 1.8 mmol) in THF (4ml) and stirred under reflux for 30 min. The resulting mixture was allowed to cool to room temperature followed by the addition of glutaric anhydride (0.128 g, 1.12 mmol) dissolved in anhydrous THF (1 mL). To this mixture  $\text{BF}_3 \cdot \text{OEt}_2$  (0.459 g, 3.24 mmol) was added slowly over 5 minutes, and allowed to stir at room temperature. After 12 h, triethylamine (1.122 g, 12 mmol) and  $\text{BF}_3 \cdot \text{OEt}_2$  (1.27 g, 9 mmol) were added and allowed to stir at 50 °C for 4 h. The reaction was quenched with ammonium chloride. The remaining precipitate dissolved in DCM and added to the aqueous solution. The mixture was then washed with water (3 x 15 mL) and extracted with  $\text{CH}_2\text{Cl}_2$  (3 x 100 mL). The organic layer was dried over  $\text{MgSO}_4$  and concentrated under nitrogen gas overnight. The oil residue was purified through a short plug using  $\text{CH}_2\text{Cl}_2$  as the eluent. After solvent evaporation, the residue obtained was further purified by preparative TLC (hexane/EtOAc/HOAc, 80:40:1) to give 151 mg of BODIPY **1** as a red solid. Yield: 50.1%. HPLC (50% A for 5 min, 10% A to 0% A over 10 min, 0% A to 50% A over 2 min at a flow rate of 4 mL/min) and  $t_R = 13.66$  min. As expected, the NMR spectral data was consistent with reported data.<sup>46</sup>

**Peptide Synthesis.** The peptide sequences GLARLLT (**2**), GYHWYGYTPQNVI (**3**), and KLARLLT (**4**), were prepared on a 0.2 mmol scale under standard Fmoc conditions and cleaved from the resin according to our previously reported procedure bearing an amide terminus.<sup>31</sup> NMR spectral data was consistent with our previously reported data.<sup>30,31</sup>

**General Procedure for Peptide Conjugation.** To a solution of carboxylic BODIPY **1** (1.5 eq) in DMF, were added TSTU (7.5 eq) and DIPEA (4 eq). The final mixture was allowed to stir for 1 h, and checked by MS for activated BODIPY. The solution was then added dropwise to a vessel containing deprotected peptide in a solution of 0.2 M  $\text{NaHCO}_3$  pH 9.2 buffer previously cooled to 0 °C for 30 min. The combined mixture was then allowed to reach 4 °C in the refrigerator, and stirred at 4 °C for an additional 24 h. The final mixture was then immediately purified using reversed phase HPLC using varying gradients of acetonitrile (solvent A) and water (solvent B) containing 0.1% TFA, as described below.

**Conjugate 5 (BODIPY-GLARLLT).** This conjugate was attained as a red orange solid (6.75 mg, 71%). HPLC (50% A for 1 min, 10% A to 0% A over 18 min, 10% A to 50% A over 2 min at a flow rate of 1 mL/min) and  $t_R = 12.82$  min.  $^1\text{H}$  NMR (500 MHz,  $\text{DMSO}-d_6$ )  $\delta$  8.03 (m, 4H), 7.84 (m, 3H), 7.41 (d, *J*

= 8.6 Hz, 3H), 7.06 (d,  $J$  = 19.2 Hz, 5H), 6.48 (s, 3H), 6.23 (s, 3H), 4.86 (d,  $J$  = 4.8 Hz, 2H), 4.28 (m, 4H), 4.07 (m, 3H), 3.75 (m, 2H), 3.67 (t,  $J$  = 6.4 Hz, 2H), 2.82 (s, 6H), 2.41 (s, 7H), 1.48 (m, 9H), 1.25 (m, 10H), 1.00 (d,  $J$  = 6.2 Hz, 4H), 0.86 (m, 18H). MS (MALDI-TOF):  $m/z$  calcd for  $C_{40}H_{78}N_{11}O_{11}$   $[M]^+$  1058.649; found 1058.648.

*Conjugate 6 (BODIPY-GYHWYGYTPQNVI)*. This conjugate was attained as a red orange solid (8.6 mg, 65 %). HPLC (50% A for 1 min, 10% A to 0% A over 18 min, 10% A to 50% A over 2 min at a flow rate of 1 mL/min) and  $t_R$  = 12.79 min.  $^1H$  NMR (500 MHz, DMSO- $d_6$ )  $\delta$  8.09 (s, 5H), 7.64 (m, 4H), 7.21 (m, 14H), 6.98 (d,  $J$  = 34.8 Hz, 10H), 6.75 (s, 2H), 6.56 (d,  $J$  = 65.7 Hz, 6H), 6.24 (s, 4H), 4.48 (d,  $J$  = 86.2 Hz, 10H), 4.05 (m, 7H), 3.67 (t,  $J$  = 6.4 Hz, 5H), 2.92 (d,  $J$  = 19.8 Hz, 10H), 2.74 (s, 9H), 2.40 (s, 8H), 1.75 (m, 9H), 1.44 (s, 3H), 1.25 (s, 8H), 1.12 (s, 7H), 0.83 (m, 18H). MS (MALDI-TOF):  $m/z$  calcd for  $C_{40}H_{78}N_{11}O_{11}$   $[M]^+$  1911.908; found 1912.793.

*Conjugate 7 (BODIPY-KLARLLT)*. This conjugate was obtained as a dark red solid (6.5 mg, 73%). HPLC (50% A for 1 min, 10% A to 0% A over 18 min, 10% A to 50% A over 2 min at a flow rate of 1 mL/min) and  $t_R$  = 9.79 min.  $^1H$  NMR (500 MHz, DMSO- $d_6$ )  $\delta$  8.27 (t,  $J$  = 5.9 Hz, 2H), 7.93 (m, 10H), 7.42 (d,  $J$  = 8.8 Hz, 2H), 7.06 (s, 2H), 6.49 (s, 5H), 6.23 (s, 3H), 4.27 (m, 5H), 4.06 (m, 6H), 3.67 (t,  $J$  = 6.4 Hz, 4H), 3.52 (s, 4H), 2.80 (m, 6H), 2.41 (s, 7H), 1.75 (m, 5H), 1.42 (s, 6H), 1.25 (s, 5H), 1.00 (d,  $J$  = 6.3 Hz, 4H), 0.86 (m, 18H). MS (MALDI-TOF):  $m/z$  calcd for  $C_{40}H_{78}N_{11}O_{11}$   $[M]^+$  1129.723; found 1129.69.

*Spectroscopy Studies*. UV-Visible and emission spectroscopy studies were measured using a Varian Cary spectrophotometer and a Perkin Elmer LS55 spectrophotometer at room temperature. Quartz cuvettes (1 cm path length) were used for each study. To analyze the data, integrated absorbance against the corresponding solution concentrations were plotted to conclude the extinction coefficients ( $\epsilon$ ) at the maximum absorption.

*SPR Studies*. Surface Plasmon Resonance analysis was conducted using extracellular domain of EGFR protein (Leinco Technologies, St. Louis, MO) immobilized on a CM5 sensor chip via standard amine coupling with a Biacore X100 (GE Healthcare Life Sciences, Marlborough MA). The running buffer used was 4 % DMSO in 1X HBS-EP+ (0.01 M HEPES, 0.15 M NaCl, 3 mM EDTA, 0.005 % Tween, pH 7.5) (GE Healthcare Biosciences), at a flow rate of 5  $\mu$ L/min. DMSO was added to the running buffer and peptide solutions to enhance the solubility of the peptides studied. The solutions were prepared in running buffer and filtered using a 0.45  $\mu$ m filter. All SPR sensorgrams relay the rates of association and dissociation of analytes at concentrations of 0 to 250  $\mu$ M performed at room temperature.



*Cell Studies.* The cells used in cytotoxicity and uptake studies was the human carcinoma HEP2 with EGFR over-expression comparable to LIM2408 colon cancer cells that are known to over-express EGFR, was purchased from the American Type Culture Collection (ATCC) (Manassas, Virginia, USA). This cell line was maintained in a 50:50 DMEM/AMEM mixture and supplemented with 5% FBS and Primocin antibiotic. To perform competitive binding experiments, the human colon cancer cell lines SW480 (129% EGFR expression), HT-29 (78% EGFR expression), DLD-1 (37% EGFR expression) and LOVO (6% EGFR expression) were also purchased from the ATCC. The HEP2 cells are often used as a model cell line in investigations of peptide-fluorophore conjugates, while the SW480 cells are a positive control for high EGFR expression (highest EGFR expression) and the LOVO cells are a negative control (lowest EGFR expression). Flow-cytometry methods using fluorescently labeled antibodies were used in the laboratory to compare the EGFR expression in the different cancer cell lines. All other reagents used in the cell studies were commercially available and purchased from Life Technologies.

*Dark Cytotoxicity.* The HEP2 cells were plated in a 96-well plate (Corning Costar) with 100  $\mu$ L medium and allowed to grow for 24 h. The stock (32 mM) solutions of the compound **1**, **5**, **6**, and **7** were prepared by using 100% DMSO as the solvent. The working solutions were prepared at 0, 6.25, 12.5, 25, 50, and 100  $\mu$ M concentrations by diluting the stock solution with culture medium. The HEP2 cells were exposed to the compound by adding 100  $\mu$ L/well of the different working solutions, five repetitions for each concentration, and incubated overnight (5% CO<sub>2</sub>, 95% humidity, 37 °C). The cells were retrieved by removal of the loading medium solution, and washed with 1X PBS solution three times. The medium with 20% CellTiter Blue (Promega) was added to the cells and allowed to incubate for another 4 h. The viability of cells were measured using a BMG FLUOstar Optima microplate reader by reading the medium fluorescence at 570/615 nm. The fluorescence intensity was normalized to 100% for the untreated cells.

**Phototoxicity.** To study phototoxicity, the HEP2 cells were exposed to each compound, **1**, **5**, **6**, and **7**, at concentrations of 100, 50, 25, 12.5, 6.25, 3.125 and 0  $\mu\text{M}$ , and incubated overnight (5%  $\text{CO}_2$ , 95% humidity, 37  $^\circ\text{C}$ ). After exposed to the compound overnight, the cells were washed with 1X PBS for three times. 100 mL of fresh medium was introduced to the cells, which were then exposed to light under a halogen lamp (600 W) light source that included a beam turning mirror (200 nm to 30  $\mu\text{m}$  spectral range, Newport) and a water filter (transmits radiation 250–950 nm), for 20 min. The cells received a total light dose of approximately 1.5  $\text{J}/\text{cm}^2$ . The cells were then incubated for another 24 h, and allowed to follow the measurement of cell viability as described above.

**Time-Dependent Cellular Uptake.** The HEP2 cells were plated at 15000 cells per well in a Costar 96-well plate (BD biosciences) and grown overnight. The cells were treated by adding 100  $\mu\text{L}$ /well of a 10  $\mu\text{M}$  working solution at different time periods of 0, 1, 2, 4, 8, and 24 h. The loading medium was removed at the end of the treatments. The cells were washed with 1X PBS, and solubilized by adding 0.25% Triton X-100 in 1X PBS. A compound standard curve, 10  $\mu\text{M}$ , 5  $\mu\text{M}$ , 2.5  $\mu\text{M}$ , 1.25  $\mu\text{M}$ , 0.625  $\mu\text{M}$ , 0.3125  $\mu\text{M}$ , was obtained by diluting stock solution with 0.25% Triton X-100 (Sigma-Aldrich) in 1X PBS. A cell standard curve was prepared using 10000, 20000, 40000, 60000, 80000, and 100000 cells per well. The cells were quantified by CyQuant Cell Proliferation Assay (Life Technologies). The compound and cell numbers were determined using a FluoStar Optima micro-plate reader (BMG LRBTEH). Cellular uptake was expressed in terms of pM/cell. For the calculation of cellular uptake: micromoles/cell =  $(C \times 100 \times 1000^{-6})/\text{cell number}$ , where C is the concentration of the compound.

**Microscopy.** The HEP2 cells were placed in 6 well plates (celltreat.com), allowed to grow overnight, and then exposed to 10  $\mu\text{M}$  concentration of the compound for 6 h. After exposure to the compound, the following organelle trackers (Invitrogen) and amounts were added to the cells: ER Tracker Blue/White (100 nM), BODIPY FL C5 Ceramide (50 nM), MitoTracker Green (250 nM), LysoSensor Green (50 nM), for 30 min in a 37  $^\circ\text{C}$  incubator. The cells were washed with 1X PBS three times, and then refilled with 1X PBS 5 mL/well. The distribution of the compounds was determined using an upright Leica DM6B fluorescence microscope fitted with standard Texas Red, GFP, DAPI, filter sets. A water immersed objective was used to determine the compound localizations.

**Competitive Binding Studies.** Different colon cancer cell lines were used based on their EGFR expressions; SW480 (high), HT-29 and DLD-1 (moderate), and LOVO (low). Competitive binding studies were carried out as described previously.<sup>29</sup> The cells were coated in a 96-well tissue culture black plate at  $10^4$  cells/well and incubated overnight at 37  $^\circ\text{C}$  with 5%  $\text{CO}_2$ . Next day, the medium was removed, and cells were treated with various concentrations (0.25 to 100  $\mu\text{M}$ ) of cyclo(K(N<sub>3</sub>)larllt)<sup>31</sup> peptide (in the

case of conjugates **5** and **7**) or YHWYGYTPQNVI peptide (in the case of conjugate **6**) with a constant concentration (50  $\mu$ M) of conjugate, in triplicate. All the compounds were diluted in phosphate buffered saline (PBS) at different concentrations. The plate was then incubated for 45 min at 37 °C with 5% CO<sub>2</sub>. After washing twice with 100  $\mu$ L of PBS, the fluorescence was measured with a microplate reader using 493 nm and 505 nm as excitation and emission wavelengths, respectively. Autofluorescence values were subtracted from each well. The average fluorescence values from triplicates were taken, and a plot of concentrations vs. relative fluorescence was plotted. For conjugate **5**, studies were carried out using only three cell lines, HT-29, DLD-1, and LOVO, because of the limited amount of the compound.

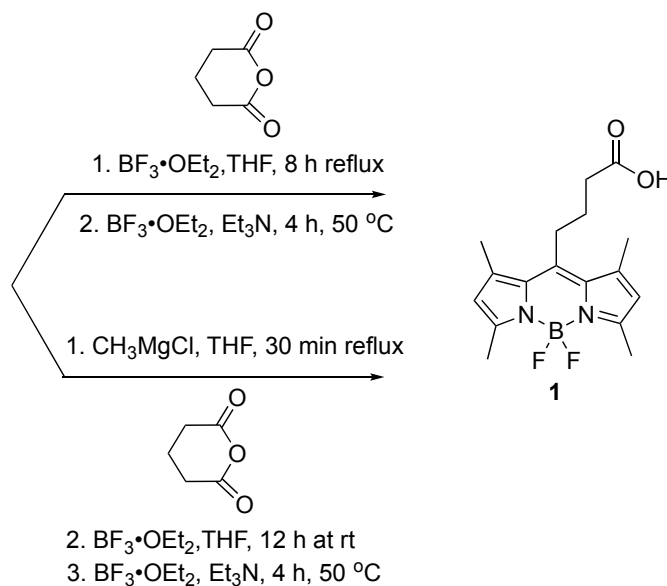
*Molecular Modeling and docking.* The structures of compounds and conjugates were created using InsightII (BIOVIA, Sandiego CA) molecular modeling software on a Linux workstation. Molecular dynamics and docking studies were carried out as described previously we described previously.<sup>23,27-31</sup> Three-dimensional structures of conjugates were subjected to molecular dynamics using simulated annealing procedure. Docking studies were conducted using AUTODOCK<sup>48</sup> with Autodock tools. The boron atom in the BODIPY moiety was replaced with carbon as parameters for boron atom are not validated in AUTODOCK 4. The EGFR protein structure (PDB ID 1nql)<sup>49</sup> was used as receptor and conjugates were used as ligands. Conjugates **5** and **7** were docked to EGFR using Lamarckian genetic algorithm and 10 million energy evaluations were performed. PyMol software (Schrödinger LLC, Portland OR) was used to represent final docked structures.

## RESULTS AND DISCUSSION

### Synthesis

The synthesis of desired starting carboxyl BODIPY **1** was designed based on the previously reported condensation of pyrroles and carboxylic anhydrides to form the corresponding carboxyl dipyrromethene, followed by coordination with BF<sub>3</sub>.OEt<sub>2</sub> under basic conditions.<sup>46</sup> This two step one-pot reaction was reported to yield carboxyl BODIPY dyes in 21-25% yields. Following this procedure the desired carboxyl BODIPY **1** was prepared from glutaric anhydride and 2,4-dimethylpyrrole. This condensation was performed in the presence of BF<sub>3</sub>.OEt<sub>2</sub> in tetrahydrofuran (THF) over the course of 8 h to promote the formation of the dipyrromethene by coordinating to the anhydride inserting a partial positive charge and ensuring the pyrrole's nucleophilic behavior. The resulting dipyrromethene was then deprotonated under basic conditions using triethylamine (TEA) and then complexed with BF<sub>3</sub>.OEt<sub>2</sub> to form carboxylic BODIPY **1**, as shown in Scheme 1. However, the purification of **1** from the reaction mixture was

challenging as multiple impurities were observed by thin layer chromatography (TLC) and as a consequence the desired product was only obtained in trace amounts (1-5%). As an effort to increase the yield of the carboxylic BODIPY **1**, microwave-assisted irradiation was applied to provide a cleaner reaction mixture at a fraction of the time, compared with conventional bench-top heating. TLC analysis did show fewer impurities, however after purification only a slight increase in yield (<10%) was obtained.



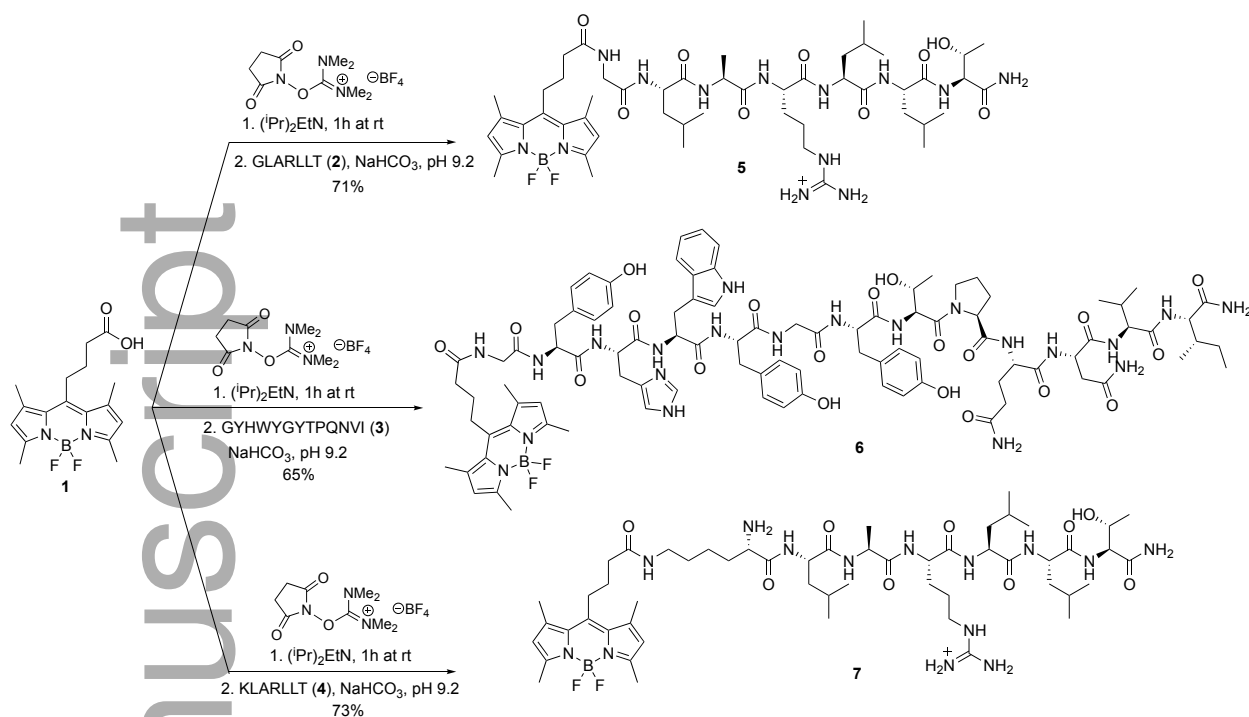
**Scheme 1.** Synthesis of carboxylic BODIPY **1** using the traditional and Grignard methodologies.

The condensation of glutaric anhydride with 2,4-dimethylpyrrole provides a short alkyl chain flanked between the core of the BODIPY dye and the point of attachment at the *meso*-position, suitable for conjugation to amino acids and proteins.<sup>46,47</sup> Ultimately, the low yields observed using glutaric anhydride are due to the low reactivity of the anhydride toward the addition of 2,4-dimethylpyrrole during the formation of the dipyrromethene, requiring an increased nucleophilicity of the pyrrole. Therefore, a Grignard of 2,4-dimethylpyrrole was created to increase its reactivity and push the reaction toward BODIPY formation.<sup>50</sup> 2,4-Dimethylpyrrole was allowed to react with methyl magnesium chloride in diethyl ether for 1 h before condensation with glutaric anhydride in THF at room temperature for 12 h, in the presence of Lewis acid  $\text{BF}_3 \cdot \text{OEt}_2$  to provide the optimal conditions for condensation of the two entities. The consequential dipyrromethene was then coordinated as before using  $\text{BF}_3 \cdot \text{OEt}_2$  and triethylamine (TEA) to yield BODIPY **1** in 50% yield after purification (Scheme 1). BODIPY **1** was characterized using  $^1\text{H}$  NMR,  $^{13}\text{C}$  NMR,  $^{11}\text{B}$  NMR and HRMS (ESI-TOF) spectroscopy techniques.

Studies have shown that peptide ligands EGFR-L1 and EGFR-L2 specifically target EGFR over-expressing tumor cells both *in vitro* and *in vivo*.<sup>9,10</sup> In our previous studies, we reported the conjugation of

EGFR-L1 or EGFR-L2 to a porphyrin,<sup>30</sup> phthalocyanine,<sup>23</sup> and a BODIPY,<sup>28,29</sup> using either short (up to 5-atom) or long (up to 20-atom) linkers. The use of linkers such as PEG groups are desired in the case of porphyrin and phthalocyanine macrocycles to increase their aqueous solubility, and potentially also for increasing their specificity for cell surface sites.<sup>51</sup> Furthermore, the use of low molecular weight PEG linkers decrease steric properties between the *N*-terminus of the peptide sequences and the photosensitizer, leading to greater yields of the desired conjugates. In the synthesis of BODIPY **1**, a short alkyl chain is released creating the “short linker effect” for conjugating to the desired peptide sequences. To further increase the distance between the BODIPY core and peptides, modified sequences of EGFR-L1 and EGFR-L2 bearing an additional glycine or lysine residue were used. Our previous findings suggest that EGFR-L1 sequence modified with a glycine or lysine spacer, as in sequences GLARLLT (**2**) and KLARLLT (**4**), does not alter the binding affinity for EGFR when compared to the parent peptide LARLLT.<sup>31</sup> A glycine was also introduced in the amino acid sequence of EGFR-L2, GYHWYGYTPQNVI (**3**), as previously reported.<sup>28</sup> Each peptide sequence was synthesized using Fmoc solid phase peptide synthesis (SPPS) chemistry on a Fmoc-Pal-PEG-PS using *N,N,N',N'*-tetramethyl-*O*-tetramethyluronium tetrafluoroborate (TBTU), 1-hydroxybenzotriazole hydrate (HOBt), and diisopropylethylamine (DIPEA) as the coupling reagents, as previously reported.<sup>23,30,52</sup> During the final step, each peptide sequences Fmoc group was removed using a 20% piperidine solution in DMF and the entire peptide sequence was then cleaved from the resin. Peptides were then collected and purified by reverse phase HPLC yielding the corresponding peptides in 37-44% yields.

Conjugation of BODIPY **1** with peptides **2**, **3**, and **4** was performed in anhydrous DMF where BODIPY **1** was activated using the coupling reagent *N,N,N',N'*-tetramethyl-*O*-(*N*-succinimidyl)uronium tetrafluoroborate (TSTU) in the presence of 1M DIPEA, at room temperature for 1 h, followed by slow addition of each peptide sequence in a 0.2 M sodium bicarbonate solution at pH 9.2 (Scheme 2). The consequential reaction mixture was stirred for 24 hours at 0°C to deliver the resultant conjugates **2**, **3** and **4** in yields of 65-73%. Reactions carried out at room temperature and/or at a higher pH provided lower conjugation yields. The BODIPY-peptide conjugates were fully characterized by <sup>1</sup>H NMR, HSQC, <sup>11</sup>B-NMR and MALDI-TOF.



**Scheme 2.** Coupling of BODIPY **1** in solution phase to peptides **2**, **3** and **4** at pH 9.2.

### Spectroscopic Properties

The maximum absorption ( $\lambda_{\text{abs}}$ ) and emission ( $\lambda_{\text{em}}$ ) wavelengths, Stokes' shifts, and molar extinction coefficients of BODIPY conjugates **5**, **6**, and **7** were investigated in dimethylsulfoxide (DMSO) solutions at room temperature, and compared to those of carboxylic BODIPY **1** precursor. The results from these studies are summarized in the Supporting Information Table S1 and Figure S1.

Carboxyl BODIPY **1** showed a characteristic strong absorption ( $\log \varepsilon = 3.97 \text{ M}^{-1}\text{cm}^{-1}$ ) at 500 nm and emission at 509 nm in DMSO, in agreement with previously reported values.<sup>46</sup> All BODIPY-peptide conjugates exhibited similar bands (absorption and emission) due to their analogous BODIPY cores, only 1 nm blue-shifted from the parent BODIPY **1**, and with slightly enhanced molar extinction coefficients. The Stokes' shifts for all BODIPY dyes, precursor and conjugates, were found to be 9 nm. These results show that conjugation of peptides to the carboxyl BODIPY does not significantly affect the characteristic spectroscopic properties of the BODIPY.

### SPR studies

The specificity of peptides **2** and **4** for EGFR was investigated in our earlier studies and determined to have a fast association and dissociation for the EGFR protein extracellular domain (ECD) through SPR studies.<sup>31</sup> To examine the binding affinity of the BODIPY-peptide conjugates to EGFR in comparison to the unconjugated BODIPY and peptide sequences, SPR<sup>53,54</sup> analysis were carried out. All BODIPY-

peptide conjugates and precursors were tested at concentrations up to 250  $\mu$ M, and the results found are shown in Figure 1a-d and in Figures S13-S15 of the Supporting Information. BODIPY **1** and conjugates **5**, **6**, and **7** were diluted to desired concentrations with a solution of running buffer HBS-EP+ containing 4% of DMSO.

BODIPY **1** showed a linear increase in response units from concentrations 50 to 200  $\mu$ M, however at 250  $\mu$ M the response begins to decrease. Furthermore, there was a sharp increase in response units in the sensorgram at all concentrations studied at 100 sec indicating the possibility of non-specific binding. Even at the lowest concentration studied (0.5  $\mu$ M) there was a sharp increase in RU suggesting non-specific binding (Figure 1a). The SPR sensorgrams for all conjugates showed a higher binding affinity for EGFR compared with that of BODIPY **1**. For conjugate **5**, saturation of binding was achieved around 100  $\mu$ M and further addition of conjugate did not increase the sensorgram stepwise (Figure 1b). Similar results were obtained for conjugate **6** (Figure 1c). However, the maximum change in RU was higher for conjugate **6** (50 RU) compared to conjugate **5** (40 RU). Conjugate **7** exhibited stepwise increase in binding from 0.5 to 250  $\mu$ M concentration with maximum increase in RU (60 RU) at 250  $\mu$ M (Figure 1d). Moreover, the sensorgram had a smooth slow increase in RU from 100 to 180 sec suggesting specific binding of conjugate to EGFR extracellular domain protein. Among the conjugates studied, **6** and **7** exhibited relatively high and specific binding to EGFR protein. Among the free peptides synthesized, GLARLLT (**2**), GYHWYGYTPQNV (**3**), and KLARLLT (**4**), peptide **4** exhibited specific and high affinity binding to EGFR extracellular domain as indicated by a stepwise increase in binding with smooth increase in RU rather than rapid increase in RU at 100 sec (see Supporting Information).

<Insert Figure 1 here>

## Cell Studies

Cellular studies were conducted using human carcinoma HEp2 cells with EGFR over-expression comparable to LIM2408 colon cancer cells<sup>55</sup> to investigate the cellular uptake, dark and phototoxicity, and subcellular distribution of BODIPY **1** and BODIPY-peptide conjugates **5**, **6**, and **7**. Colon cancer cell lines with high EGFR expression (SW480), moderate EGFR expression (HT-29 and DLD-1), and low EGFR expression (LOVO) were used in the competitive binding studies for the competitive binding experiments.<sup>56</sup>

*Cytotoxicity.* The dark and phototoxic effects of BODIPY **1** and its peptide conjugates **5**, **6**, and **7** were evaluated in HEp2 cells using a Cell Titer Blue (CTB) assay and low light dose of 1.5 J/cm<sup>2</sup>. The results attained are shown in Table 1 and in Figures S2 and S3 of the Supporting Information. No dark nor phototoxicity were observed for BODIPY **1** and its conjugates **5**, **6**, and **7** with IC<sub>50</sub> values greater than 200 μM (dark) and 100 μM (light, 1.5 J/cm<sup>2</sup>). These results are not surprising, as the BODIPY core is intrinsically non-phototoxic, unless substituted with heavy atoms and/or certain moieties that can modulate its toxic effects.<sup>57</sup>

<Insert Table 1 here>

*Time-dependent cellular uptake.* The evaluation of BODIPY **1** and its peptide conjugates **5**, **6**, and **7** were time-dependent cellular uptake studies performed at 10 μM concentration in HEp2 cells over a 24 h period, and the results are shown in Figure 2. Conjugate **6** bearing the EGFR-L2 peptide sequence GYHWYGYTPQNVI accumulated the most within cells of all other BODIPYs at all time points investigated. At 24 h the amount of conjugate **6** taken up by cells was approximately 5-fold that of BODIPY **1** (see Table S2 in the Supporting Information). On the other hand, BODIPY **1** and its conjugates to the modified EGFR-L1 sequences, **5** and **7**, showed similar uptake into the HEp2 cells. This result was surprising as we anticipated that the peptide conjugates would show enhanced cellular uptake relative to the carboxyl BODIPY **1**, as previously observed.<sup>29,31</sup> This might be a result of the much smaller size of BODIPY **1** which favors passive diffusion across the cellular membrane, increasing its cellular uptake. On the other hand, the smaller size of the BODIPY core in conjugate **6** may enhance its binding ability to the EGF binding pocket on the EGFR ECD (see below).

<Insert Figure 2 here>



*Subcellular Localization.* The preferential sites of localization were determined using fluorescence microscopy on BODIPY conjugates **5-7** in HEp2 cells, and the findings are displayed in Table 1 and in Figures 3, 4 and 5. The images obtained with the carboxyl BODIPY **1** are shown in Figure S5 of the Supporting Information. Co-localization studies using fluorescent trackers specific to organelles including ERTracker Blue/White (endoplasmic reticulum), LysoSensor Green (lysosomes), MitoTracker Green (mitochondria), and BODIPY FL C5 Ceramide (Golgi) were performed. All conjugates were found to preferably localize in the cell lysosomes, as seen by the orange/yellow color in Figures 3j, 4j and 5j. Additionally, the EGFR-L1 containing conjugates **5** and **6**, as well as BODIPY **1** were also found to also localize in the cell mitochondria, while the EGFR-L2 containing conjugate **6** was also found in the ER.

<Insert Figure 3 here>

<Insert Figure 4 here>

<Insert Figure 5 here>

*Competitive Binding Studies.* To investigate the specificity of the BODIPY-peptide conjugates for binding to the EGFR over-expressed on cancer cells, competitive binding studies were conducted using unlabeled cyclo(K(N3)larllt)<sup>31</sup> peptide. These studies were carried out using four cell lines with differential EGFR expression: SW480, HT-29, DLD-1 and LOVO (high to low EGFR expression).<sup>56</sup> For the competitive binding studies of conjugates **5** and **7** bearing the EGFR-L1 peptide, a cyclic version was used, cyclo(K(N3)larllt), previously shown to bind to EGFR with high affinity.<sup>31</sup> For conjugate **6** unlabeled EGFR-L2 peptide was used for the competitive binding studies. The results obtained are shown in Figures 6 and 7, and in Figure S4 of the Supporting Information. For all conjugates the addition of unlabeled peptide resulted in a decrease of the fluorescence intensity, suggesting that the unlabeled peptide can displace the conjugate bound to EGFR on the cells' surface. When conjugate **6** was incubated with unlabeled EGFR-L2 peptide at concentrations up to 100  $\mu$ M, a clear dose-dependent decrease in fluorescence was observed in all cell lines, particularly those with high and moderate EGFR expression (SW480, HT-29 and DLD-1) as seen in Figure 6. In the case of conjugates **5** and **7** bearing the EGFR-L1 peptide, the fluorescence intensity did not decreased as significantly upon addition of unlabeled cyclo(K(N3)larllt) peptide (Figures 7 and S4 in the Supporting Information). Particularly in the case of **5** the fluorescence intensity appears to level off upon addition of 0.5  $\mu$ M of unlabeled peptide, which suggests some non-specific binding of this conjugate. For LOVO with low EGF expression, when unlabeled peptide was added, labeled peptide was displaced and there was no concentration dependence of competitive binding indicating non-specific binding of conjugate to the cell surface. These results indicate that conjugate **6** bearing the GYHWYGYTPQNVI (**3**) peptide binds to EGFR with greater specificity among all the conjugates. On the other hand, the SPR results suggested that conjugates **6** and **7** bound to the EGFR extracellular domain with specificity compared to that of conjugate **5**. Since the SPR studies were carried out with purified EGFR protein immobilized on a CM5 chip, we believe that the condition of immobilized protein and protein on the cell surface in the native environment are slightly different and hence there is a difference in the results obtained from the SPR and competitive binding studies.

<Insert Figure 6 here>

<Insert Figure 7 here>

## Modeling and Docking

To envision the interactions of the BODIPY-peptide conjugates with EGFR ECD, the 3D structures of **5**, **6** and **7** were generated and docked to the EGFR closed conformation using AUTODOCK. The EGFR-L1

peptide is known to bind to domain I of the EGFR ECD<sup>9,23,31</sup> and hence conjugates **5** and **7** were docked on this domain. On the other hand EGFR-L2 peptide is known to bind close to the EGF binding pocket between domains I and III of the EGFR ECD<sup>10,23</sup> and hence conjugate **6** was docked near the EGF binding pocket. The docking studies suggest that conjugate **5** bearing the GLARLLT peptide binds to domain I of EGFR with a docking energy of -9.68 kcal/mol (Figure 8A). In the docked position, extended from the peptide, the BODIPY moiety also binds to the EGFR protein near Leu225, Val226, Gln81 and Gln59. The peptide part of the conjugate has interactions with Thr217, Arg200, Leu186, Gln184, Glu180 of EGFR. Conjugate **7** also bearing the KLARLLT peptide also binds to EGFR domain 1 with a docking energy of -6.61 kcal/mol. In the case of this conjugate the BODIPY moiety is near the hydrophobic binding pocket formed by Pro171 and alkyl side chains of Lys201 and Leu186. The peptide part of conjugate **7** forms hydrogen bonds as well as hydrophobic interactions with the EGFR protein and it is surrounded by amino acid residues Arg200, Lys201, Lys185, Leu 186 and Leu225 (Figure 8B). On the other hand, conjugate **6** bearing the GYHWYGYTPQNVI peptide binds near the EGF binding pocket between domains I and III of EGFR ECD with a docking energy of -9.97 kcal/mol (Figure 8C). The BODIPY moiety faces the helical structure of EGFR and forms hydrophobic interactions with Ile370 of EGFR. These results are consistent with the SPR binding and the competitive binding studies which suggest that in addition to the peptide interactions in conjugates **5**, **6** and **7**, the BODIPY moiety also binds to EGFR non-specifically, by forming multiple hydrophobic interactions with the EGFR ECD. Furthermore, conjugate **6** bearing the GYHWYGYTPQNVI peptide was found to bind with the lowest docking energy of all conjugates near the EGF binding pocket, suggesting high specificity for this conjugate.

<Insert Figure 8 here>

## CONCLUSIONS

In this work we have optimized the synthesis of a carboxyl BODIPY dye, which can be readily conjugated to amino acids, peptides and proteins via amide bond formation. This BODIPY was conjugated under mild conditions in yields up to 75% to EGFR-targeting peptides GLARLLT, KLARLLT, and GYHWYGYTPQNVI. All BODIPY conjugates were characterized using <sup>1</sup>H NMR, <sup>11</sup>B NMR, HSQC NMR, mass spectrometry (MALDI-TOF), UV-Vis and fluorescence spectroscopies. Using AUTODOCK, all conjugates were found to bind to EGFR ECD with negative docking energies. While peptides GLARLLT and KLARLLT bind to domain I of EGFR protein away from the EGF binding pocket, the GYHWYGYTPQNVI peptide binds between domains I and III, close to the EGF binding pocket. The BODIPY moiety also binds non-specifically to EGFR, forming hydrophobic interactions with

several residues. SPR studies indicated that the conjugates exhibited both specific and non-specific binding to EGFR. Competitive binding studies revealed a dose-dependent decrease in fluorescence in four cell lines with different EGFR expression, particularly for conjugate **6** bearing the GYHWYGYTPQNVI peptide. Cytotoxicity studies using human carcinoma HEp2 cells revealed no dark ( $IC_{50} > 200 \mu M$ ) nor phototoxicity ( $IC_{50} > 100 \mu M$ ,  $1.5 J/cm^2$ ) for all the BODIPYs. Conjugate **6** bearing the GYHWYGYTPQNVI peptide accumulated the most within HEp2 cells at all time points investigated up to 24 h, showing ~ 5-fold higher accumulation than the other conjugates and unconjugated BODIPY. All conjugates localized intracellularly preferentially in the lysosomes, and in addition conjugate **6** was also observed in the ER while conjugates **5** and **7** were also found in the cell mitochondria. Our results indicate that BODIPY-peptide conjugate **6** is the most efficient at targeting the EGFR ECD and it is a promising fluorescence imaging agent for EGFR-overexpressing tumors such as CRC.

### Acknowledgements

This work was supported by the National Science Foundation, grant number CHE 1800126, and the National Institutes of Health, grant number R01 CA179902. Computational studies were performed using HPC resources at Louisiana State University, Baton Rouge, via LONI. The BBC core of LBRN is acknowledged for the use of the computational facility.

### SUPPORTING INFORMATION

Additional supporting information may be found online in the Supporting Information section at the end of the article:

Figures S1 to S37 and Tables S1 and S2 contain spectroscopic data, cytotoxicity, cellular uptake, competitive binding of conjugate **5**, subcellular localization, HPLC traces, SPR analysis, copies of MALDI(TOF) & MALDI(TOF-TOF), copies of  $^1H$  NMR spectra, copies of HSQC, and copies of  $^{11}B$  NMR spectra.

### REFERENCES

1. Sovich, J. L.; Sartor, Z.; Misra, S., Developments in Screening Tests and Strategies for Colorectal Cancer. *BioMed Research International* **2015**, 326728.

2. Kiesslich, R.; Goetz, M.; Vieth, M.; Galle, P. R.; Neurath, M. F., Technology Insight: confocal laser endoscopy for in vivo diagnosis of colorectal cancer. *Nat. Clin. Prac. Oncol.* **2007**, *4* (8), 480-490.
3. Hoffman, A.; Goetz, M.; Vieth, M.; Galle, P.; Neurath, M.; Kiesslich, R., Confocal laser endomicroscopy: technical status and current indications. *Endoscopy* **2006**, *38* (12), 1275-1283.
4. Dolmans, D. E.; Fukumura, D.; Jain, R. K., Photodynamic therapy for cancer. *Nature Rev. Cancer* **2003**, *3* (5), 380-387.
5. Tomas, A.; Futter, C. E.; Eden, E. R., EGF receptor trafficking: consequences for signaling and cancer. *Trends Cell Biol.* **2014**, *24* (1), 26-34.
6. Yewale, C.; Baradia, D.; Vhora, I.; Patil, S.; Misra, A., Epidermal growth factor receptor targeting in cancer: A review of trends and strategies. *Biomaterials* **2013**, *34* (34), 8690-8707.
7. Hynes, N. E.; Lane, H. A., ERBB receptors and cancer: the complexity of targeted inhibitors. *Nat. Rev. Cancer* **2005**, *5* (5), 341-354.
8. Burgess, A. W.; Cho, H.-S.; Eigenbrot, C.; Ferguson, K. M.; Garrett, T. P. J.; Leahy, D. J.; Lemmon, M. A.; Sliwkowski, M. X.; Ward, C. W.; Yokoyama, S., An Open-and-Shut Case? Recent Insights into the Activation of EGF/ErbB Receptors. *Mol. Cell* **2003**, *12* (3), 541-552.
9. Song, S.; Liu, D.; Peng, J.; Deng, H.; Guo, Y.; Xu, L. X.; Miller, A. D.; Xu, Y., Novel peptide ligand directs liposomes toward EGF-R high-expressing cancer cells in vitro and in vivo. *The FASEB Journal* **2009**, *23* (5), 1396-1404.
10. Li, Z.; Zhao, R.; Wu, X.; Sun, Y.; Yao, M.; Li, J.; Xu, Y.; Gu, J., Identification and characterization of a novel peptide ligand of epidermal growth factor receptor for targeted delivery of therapeutics. *The FASEB Journal* **2005**, *19* (14), 1978-1985.
11. Oda, K.; Matsuoka, Y.; Funahashi, A.; Kitano, H., A comprehensive pathway map of epidermal growth factor receptor signaling. *Mol. Syst. Biol.* **2005**, *1* (1), 2005.0010.
12. Bhirde, A. A.; Patel, V.; Gavard, J.; Zhang, G.; Sousa, A. A.; Masedunskas, A.; Leapman, R. D.; Weigert, R.; Gutkind, J. S.; Rusling, J. F., Targeted killing of cancer cells in vivo and in vitro with EGF-directed carbon nanotube-based drug delivery. *ACS Nano* **2009**, *3* (2), 307-316.
13. Patra, C. R.; Bhattacharya, R.; Wang, E.; Katarya, A.; Lau, J. S.; Dutta, S.; Muders, M.; Wang, S.; Buhrow, S. A.; Safgren, S. L.; Yaszemski, M. J.; Reid, J. M.; Ames, M. M.; Mukherjee, P.; Mukhopadhyay, D., Targeted delivery of gemcitabine to pancreatic adenocarcinoma using cetuximab as a targeting agent. *Cancer Res.* **2008**, *68* (6), 1970-1978.
14. Saki, M.; Toulany, M.; Sihver, W.; Zenker, M.; Heldt, J.-M.; Mosch, B.; Pietzsch, H.-J.; Baumann, M.; Steinbach, J.; Rodemann, H. P., Cellular and molecular properties of 90Y-labeled cetuximab in combination with radiotherapy on human tumor cells in vitro. *Strahlentherapie Onkol.* **2012**, *188* (9), 823-832.

15. Leonidova, A.; Foerster, C.; Zarschler, K.; Schubert, M.; Pietzsch, H.-J.; Steinbach, J.; Bergmann, R.; Metzler-Nolte, N.; Stephan, H.; Gasser, G., In vivo demonstration of an active tumor pretargeting approach with peptide nucleic acid bioconjugates as complementary system. *Chem. Sci.* **2015**, *6* (10), 5601-5616.
16. Yang, L.; Mao, H.; Wang, Y. A.; Cao, Z.; Peng, X.; Wang, X.; Duan, H.; Ni, C.; Yuan, Q.; Adams, G.; Smith, M. Q.; Wood, W. C.; Gao, X.; Nie, S., Single chain epidermal growth factor receptor antibody conjugated nanoparticles for in vivo tumor targeting and imaging. *Small* **2009**, *5* (2), 235-243.
17. Sexton, K.; Tichauer, K.; Samkoe, K. S.; Gunn, J.; Hoopes, P. J.; Pogue, B. W., Fluorescent affibody peptide penetration in glioma margin is superior to full antibody. *PLoS ONE* **2013**, *8* (4), e60390.
18. Nordberg, E.; Friedman, M.; Göstring, L.; Adams, G. P.; Brismar, H.; Nilsson, F. Y.; Ståhl, S.; Glimelius, B.; Carlsson, J., Cellular studies of binding, internalization and retention of a radiolabeled EGFR-binding affibody molecule. *Nuclear Med. Biol.* **2007**, *34* (6), 609-618.
19. Bell, A.; Wang, Z. J.; Arbabi-Ghahroudi, M.; Chang, T. A.; Durocher, Y.; Trojahn, U.; Baardsnes, J.; Jaramillo, M. L.; Li, S.; Baral, T. N.; O'Connor-McCourt, M.; MacKenzie, R.; Zhang, J., Differential tumor-targeting abilities of three single-domain antibody formats. *Cancer Lett.* **2010**, *289* (1), 81-90.
20. Mickler, F. M.; Möckl, L.; Ruthardt, N.; Ogris, M.; Wagner, E.; Bräuchle, C., Tuning nanoparticle uptake: live-cell imaging reveals two distinct endocytosis mechanisms mediated by natural and artificial EGFR targeting ligand. *Nano Lett.* **2012**, *12* (7), 3417-3423.
21. Chariou, P. L.; Lee, K. L.; Wen, A. M.; Gulati, N. M.; Stewart, P. L.; Steinmetz, N. F., Detection and imaging of aggressive cancer cells using an epidermal growth factor receptor (EGFR)-targeted filamentous plant virus-based nanoparticle. *Bioconjugate Chem.* **2015**, *26* (2), 262-269.
22. Zarschler, K.; Prapainop, K.; Mahon, E.; Rocks, L.; Bramini, M.; Kelly, P. M.; Stephan, H.; Dawson, K. A., Diagnostic nanoparticle targeting of the EGF-receptor in complex biological conditions using single-domain antibodies. *Nanoscale* **2014**, *6* (11), 6046-6056.
23. Ongarora, B. G.; Fontenot, K. R.; Hu, X.; Sehgal, I.; Satyanarayana-Jois, S. D.; Vicente, M. G. H., Phthalocyanine-peptide conjugates for epidermal growth factor receptor targeting. *J. Med. Chem.* **2012**, *55* (8), 3725-3738.
24. Hamzeh-Mivehroud, M.; Mahmoudpour, A.; Dastmalchi, S., Identification of new peptide ligands for epidermal growth factor receptor using phage display and computationally modeling their mode of binding. *Chem Biol Drug Des* **2012**, *79*, 246-259.
25. Franek, J.; Cappelleri, J. C.; Larkin-Kaiser, K. A.; Wilner, K. D.; Sandin, R., Systematic review and network meta-analysis of first-line therapy for advanced EGFR-positive non-small-cell lung cancer. *Future Oncology*, **2019**, *15* (24), 2857-2871.

26. Viehweger, K.; Barbaro, L.; García, K. P.; Joshi, T.; Geipel, G.; Steinbach, J.; Stephan, H.; Spiccia, L.; Graham, B., EGF Receptor-targeting peptide conjugate incorporating a near-IR fluorescent dye and a novel 1,4,7-triazacyclononane-based  $^{64}\text{Cu}(\text{II})$  chelator assembled via click chemistry. *Bioconjugate Chem.* **2014**, *25* (5), 1011-1022.
27. Banappagari, S.; McCall, A.; Fontenot, K.; Vicente, M. G. H.; Gujar, A.; Satyanarayanajois, S., Design, synthesis and characterization of peptidomimetic conjugate of BODIPY targeting HER2 protein extracellular domain. *Eur. J. Med. Chem.* **2013**, *65*, 60-69.
28. Zhao, N.; Williams, T. M.; Zhou, Z.; Fronczek, F. R.; Sibrian-Vazquez, M.; Jois, S. D.; Vicente, M. G. H., Synthesis of BODIPY-peptide conjugates for fluorescence labeling of EGFR overexpressing cells. *Bioconjugate Chem.* **2017**, *28* (5), 1566–1579.
29. Kauffman, N. E.; Meng, Q.; Griffin, K. E.; Singh, S. S.; Dahal, A.; Zhou, Z.; Fronczek, F. R.; Mathis, J. M.; Jois, S. D.; Vicente, M. G. H., Synthesis, characterization, and evaluation of near-IR boron dipyrromethene bioconjugates for labeling of adenocarcinomas by selectively targeting the epidermal growth factor receptor. *J. Med. Chem.* **2019**, *62* (7), 3323-3335.
30. Fontenot, K. R.; Ongarora, B. G.; LeBlanc, L. E.; Zhou, Z.; Jois, S. D.; Vicente, M. G. H., Targeting of the epidermal growth factor receptor with mesoporphyrin IX-peptide conjugates. *J. Porphyrins Phthalocyanines* **2016**, *20* (01n04), 352-366.
31. Williams, T. M.; Sable, R.; Singh, S.; Vicente, M. G. H.; Jois, S. D., Peptide ligands for targeting the extracellular domain of EGFR: Comparison between linear and cyclic peptides. *Chem. Biol. Drug Design* **2018**, *91* (2), 605-619.
32. Ulrich, G.; Ziessel, R.; Harriman, A., The chemistry of fluorescent BODIPY dyes: versatility unsurpassed. *Angew. Chem. Int. Ed.* **2008**, *47* (7), 1184-1201.
33. Ge, Y.; O'Shea, D. F., Azadipyrromethenes: from traditional dye chemistry to leading edge applications. *Chem. Soc. Rev.* **2016**, *45* (14), 3846-3864.
34. Lakshmi, V.; Rajeswara Rao, M.; Ravikanth, M., Halogenated boron-dipyrromethenes: synthesis, properties and applications. *Org. Biomol. Chem.* **2015**, *13* (9), 2501-2517.
35. Loudet, A.; Burgess, K., BODIPY dyes and their derivatives: syntheses and spectroscopic properties. *Chem. Rev.* **2007**, *107* (11), 4891-4932.
36. Lu, H.; Mack, J.; Yang, Y.; Shen, Z., Structural modification strategies for the rational design of red/NIR region BODIPYs. *Chem. Soc. Rev.* **2014**, *43* (13), 4778-4823.
37. Jang, H. G.; Park, M.; Wishnok, J. S.; Tannenbaum, S. R.; Wogan, G. N., Hydroxyl-specific fluorescence labeling of ABP-deoxyguanosine, PhIP-deoxyguanosine, and AFB1-formamidopyrimidine with BODIPY-FL. *Anal. Biochem.* **2006**, *359* (2), 151-160.

38. Yee, M.-c.; Fas, S. C.; Stohlmeyer, M. M.; Wandless, T. J.; Cimprich, K. A., A cell-permeable, activity-based probe for protein and lipid kinases. *J. Biol. Chem.* **2005**, *280* (32), 29053-29059.
39. Skidmore, M.; Guimond, S.; Dumax-Vorzet, A.; Atrih, A.; Yates, E.; Turnbull, J., High sensitivity separation and detection of heparan sulfate disaccharides. *J. Chromat. A* **2006**, *1135* (1), 52-56.
40. Aharoni, A.; Weiner, L.; Lewis, A.; Ottolenghi, M.; Sheves, M., Nonisomerizable non-retinal chromophores initiate light-induced conformational alterations in bacterioopsin. *J. Am. Chem. Soc.* **2001**, *123* (27), 6612-6616.
41. Rezende, L. C.; Emery, F. S., A review of the synthetic strategies for the development of BODIPY dyes for conjugation with proteins. *Orb. Elect. J. Chem.* **2013**, *5* (1), 62-83.
42. Ni, Y.; Zeng, L.; Kang, N. Y.; Huang, K. W.; Wang, L.; Zeng, Z.; Chang, Y. T.; Wu, J., meso - Ester and carboxylic acid substituted BODIPYs with far - red and near - infrared emission for bioimaging applications. *Chem. Eur. J.* **2014**, *20* (8), 2301-2310.
43. Ducheyne, P.; Healy, K.; Hutmacher, D. E.; Grainger, D. W.; Kirkpatrick, C. J., *In Comprehensive biomaterials*. 1st Ed.; Elsevier Science: **2011**; Vol. 1.
44. Spicka, K. J., *Design and synthesis of fluorescent dyes for use in proteomic research*. ProQuest: **2008**.
45. Lavis, L. D., *Tailoring fluorescent molecules for biological applications*. ProQuest: **2008**.
46. Wang, D.; Fan, J.; Gao, X.; Wang, B.; Sun, S.; Peng, X., Carboxyl BODIPY dyes from bicarboxylic anhydrides: one-pot preparation, spectral properties, photostability, and biolabeling. *J. Org. Chem.* **2009**, *74* (20), 7675-7683.
47. Ksenofontova, K. V.; Ksenofontov, A. A.; Khodov, I. A.; Rumyantsev, E. V., Novel BODIPY-conjugated amino acids: synthesis and spectral properties. *J. Mo. Liquids* **2019**, *283*, 695-703.
48. Morris, G. M.; Huey, R.; Lindstrom, W.; Sanner, M. F.; Belew, R. K.;Goodsell, D. S.; Olson, A. J., AutoDock4 and AutoDockTools4: Automated docking with selective receptor flexibility. *J. Comput. Chem.* **2009**, *30* (16), 2785-2791.
49. Ferguson, K. M.; Berger, M. B.; Mendrola, J. M.; Cho, H.-S.; Leahy, D. J.; Lemmon, M. A., EGF activates its receptor by removing interactions that autoinhibit ectodomain dimerization. *Mol. Cell* **2003**, *11* (2), 507-517.
50. Tahtaoui, C.; Thomas, C.; Rohmer, F.; Klotz, P.; Duportail, G.; Mély, Y.; Bonnet, D.; Hibert, M., Convenient method to access new 4, 4-dialkoxy-and 4, 4-diaryloxy-diaza-s-indacene dyes: Synthesis and spectroscopic evaluation. *J. Org. Chem.* **2007**, *72* (1), 269-272.
51. Hermanson, G. T., *Bioconjugate techniques*. 3<sup>rd</sup> Ed.; Academic press: New York, **2013**.
52. Merrifield, R. B., Solid phase peptide synthesis. I. The synthesis of a tetrapeptide. *J. Am. Chem. Soc.* **1963**, *85* (14), 2149-2154.



53. Komolov, K. E.; Koch, K.-W., Application of surface plasmon resonance spectroscopy to study G-protein coupled receptor signalling. In *Surface Plasmon Resonance: Methods and Protocols*, Mol, N. J.; Fischer, M. J. E., Eds. Humana Press: Totowa, NJ, **2010**; pp 249-260.
54. Wilson, W. D., Analyzing biomolecular interactions. *Science* **2002**, *295* (5562), 2103-2105.
55. Liu, F.; Zhu, Y.; Qian, Y.; Zhao, Y.; Zhao, X.; Zhang, J.; Zhang, Y.; Zhang Y., Effects of gold nanorods modified with antiepidermal growth factor receptor monoclonal antibody on laryngeal cancer cells. *Turk J. Biol.* **2018**, *42* (2), 144-151.
56. Yang, J. L.; Qu, X. J.; Russell, P. J.; Goldstein, D., Regulation of epidermal growth factor receptor in human colon cancer cell lines by interferon alpha. *Gut.* **2004**, *53* (1), 123-129.
57. Gibbs, J. H.; Robins, L. T.; Zhou, Z.; Bobadova-Parvanova, P.; Cottam, M.; McCandless, G. T.; Fronczek, F. R.; Vicente, M. G. H., Spectroscopic, computational modeling and cytotoxicity of a series of meso-phenyl and meso-thienyl-BODIPYs. *Bioorg. Med. Chem.* **2013**, *21* (18), 5770-5781.

## Tables

**Table 1.** Cytotoxicity for BODIPYs **1**, **5**, **6** and **7** using a Cell Titer Blue assay (1.5 J/cm<sup>2</sup> light dose), and their major localization sites in human carcinoma HEP2 cells.

| Compound | Dark toxicity<br>(IC <sub>50</sub> , μM ) | Phototoxicity<br>(IC <sub>50</sub> , μM ) | Major sites of localization |
|----------|---|---|-----------------------------|
| <b>1</b> | > 200                                     | >100                                      | ER, Mito                    |
| <b>5</b> | > 200                                     | >100                                      | ER, Mito, Lyso              |
| <b>6</b> | > 200                                     | >100                                      | ER, Lyso                    |
| <b>7</b> | > 200                                     | >100                                      | ER, Mito, Lyso              |

## Figures

**Figure 1.** SPR sensorgrams for BODIPY **1** (a) and its peptide conjugates **5** (b), **6** (c), and **7** (d) at concentrations up to 250  $\mu$ M. Blank (mint), 0.5  $\mu$ M (purple), 1  $\mu$ M (navy blue), 10  $\mu$ M (royal blue), 25  $\mu$ M (green), 50  $\mu$ M (orange), 100  $\mu$ M (yellow), 200  $\mu$ M (lime), and 250  $\mu$ M (burgundy).

**Figure 2.** Cellular Uptake of BODIPY **1** (black) and its peptide conjugates **5** (green), **6** (pink), **7** (purple) in human HEp2 cells.

**Figure 3.** Fluorescence microscopy of BODIPY-peptide conjugate **5** in human carcinoma HEp2 cells at 10  $\mu$ M for 6 h. (a) Phase contrast; (b) overlay of phase contrast and fluorescence of **5**. Fluorescence of organelle tracers (c) ER Tracker Blue/White, (e) BODIPY Ceramide, (g) MitoTracker Green, and (i) LysoSensor Green. (d,f,h,j) Overlay of organelle tracer and **5** fluorescence. Scale bar: 10  $\mu$ m.

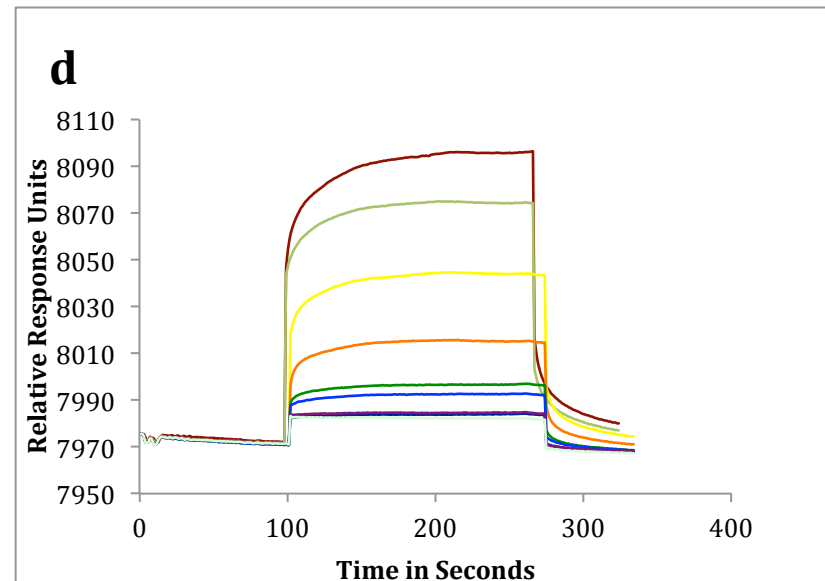
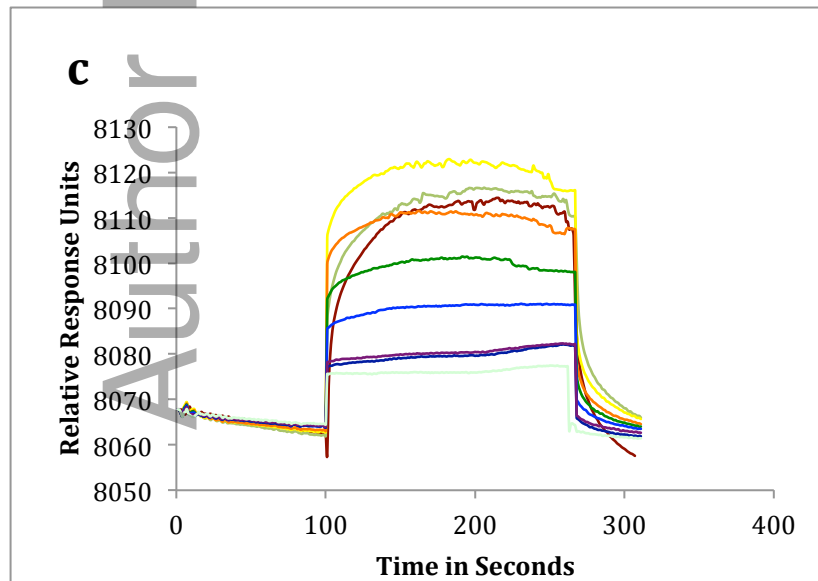
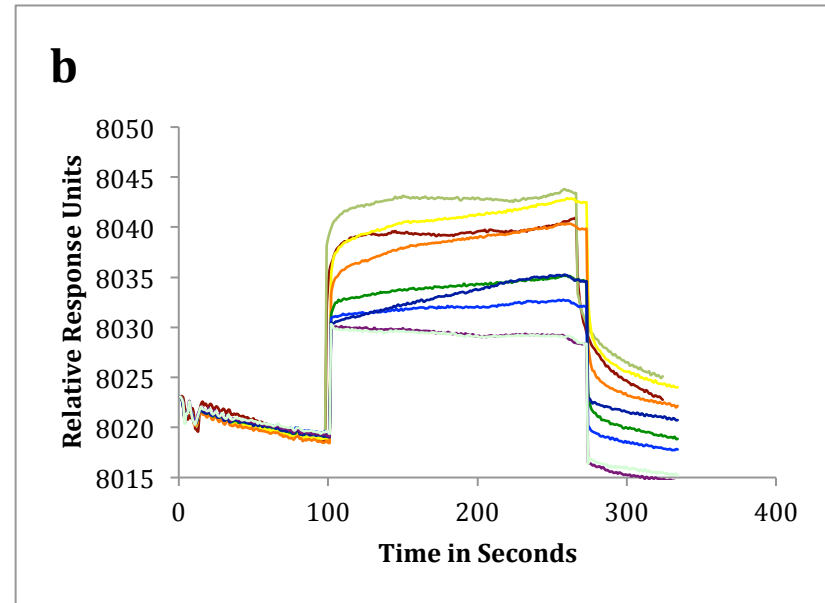
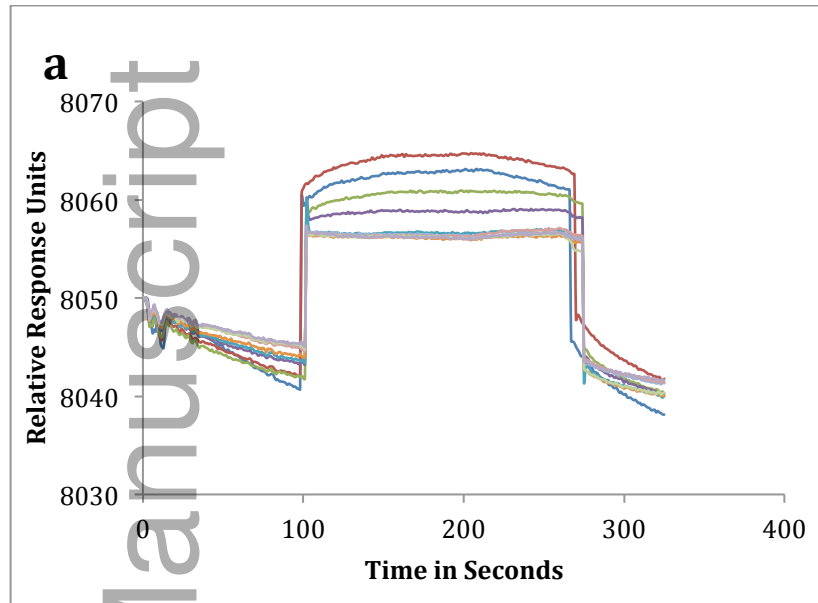
**Figure 4.** Fluorescence microscopy of BODIPY-peptide conjugate **6** in human carcinoma HEp2 cells at 10  $\mu$ M for 6 h. (a) Phase contrast; (b) overlay of phase contrast and fluorescence of **6**. Fluorescence of organelle tracers (c) ER Tracker Blue/White, (e) BODIPY Ceramide, (g) MitoTracker Green, and (i) LysoSensor Green. (d,f,h,j) Overlay of organelle tracer and **6** fluorescence. Scale bar: 10  $\mu$ m.

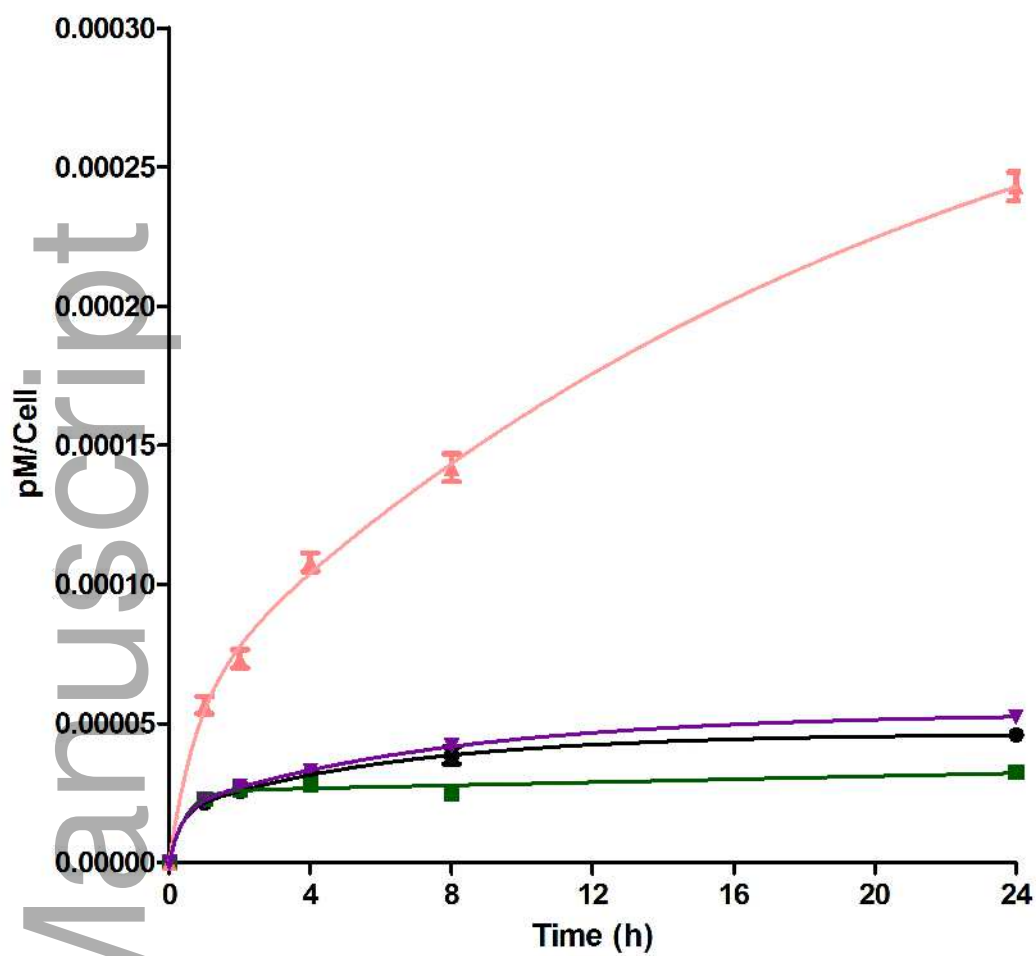
**Figure 5.** Fluorescence microscopy of BODIPY-peptide conjugate **7** in human carcinoma HEp2 cells at 10  $\mu$ M for 6 h. (a) Phase contrast; (b) overlay of phase contrast and **7** fluorescence. Fluorescence of organelle tracers (c) ER Tracker Blue/White, (e) BODIPY Ceramide, (g) MitoTracker Green, and (i) LysoSensor Green. (d,f,h,j) Overlay of organelle tracer and **7** fluorescence. Scale bar: 10  $\mu$ m.

**Figure 6.** Competitive binding of BODIPY-peptide conjugate **6** with unlabeled EGFR-L2 peptide. Binding of **6** to A) SW480 cells (high EGFR expression), B) and C) HT-29, DLD-1 (moderate EGFR expression), D) LOVO (low EGFR expression).

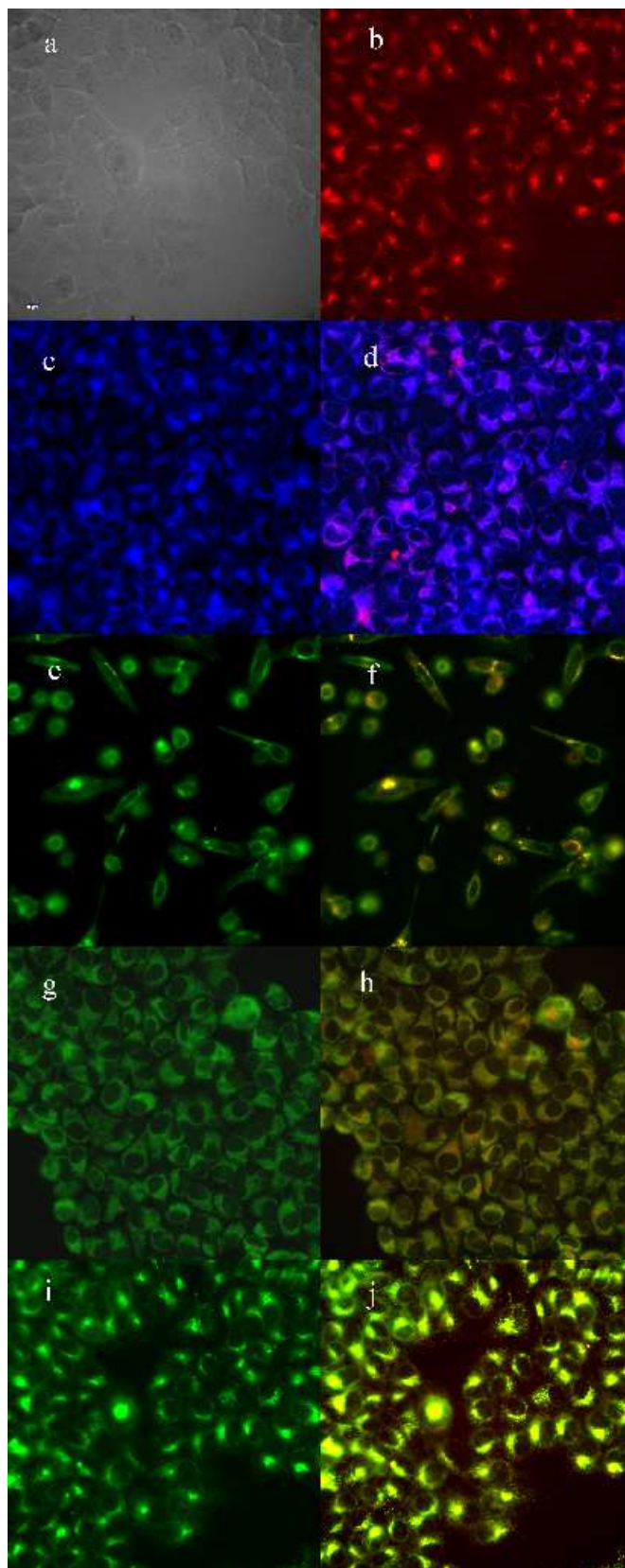
**Figure 7.** Competitive binding of BODIPY-peptide conjugate **7** with cyclo(K(N3)larllt). Binding of **7** to A) SW480 cells (high EGFR expression), B) and C) HT-29, DLD-1 (moderate EGFR expression), D) LOVO (low EGFR expression).

**Figure 8.** Model of interaction of BODIPY-peptide conjugates **5** (A), **7** (B) and **6** (C) with EGFR protein using Autodock. The lowest energy docked structures are represented. The extracellular domains I and II of EGFR (PDB ID 1NQL) are shown as surface representation, the conjugates are shown as sticks and the BODIPY moiety is highlighted with a rectangle. Hydrophobic interactions are shown in blue and polar interactions are shown in red. Amino acids of EGFR are represented by three letters, and those on the peptide are indicated by a single letter.

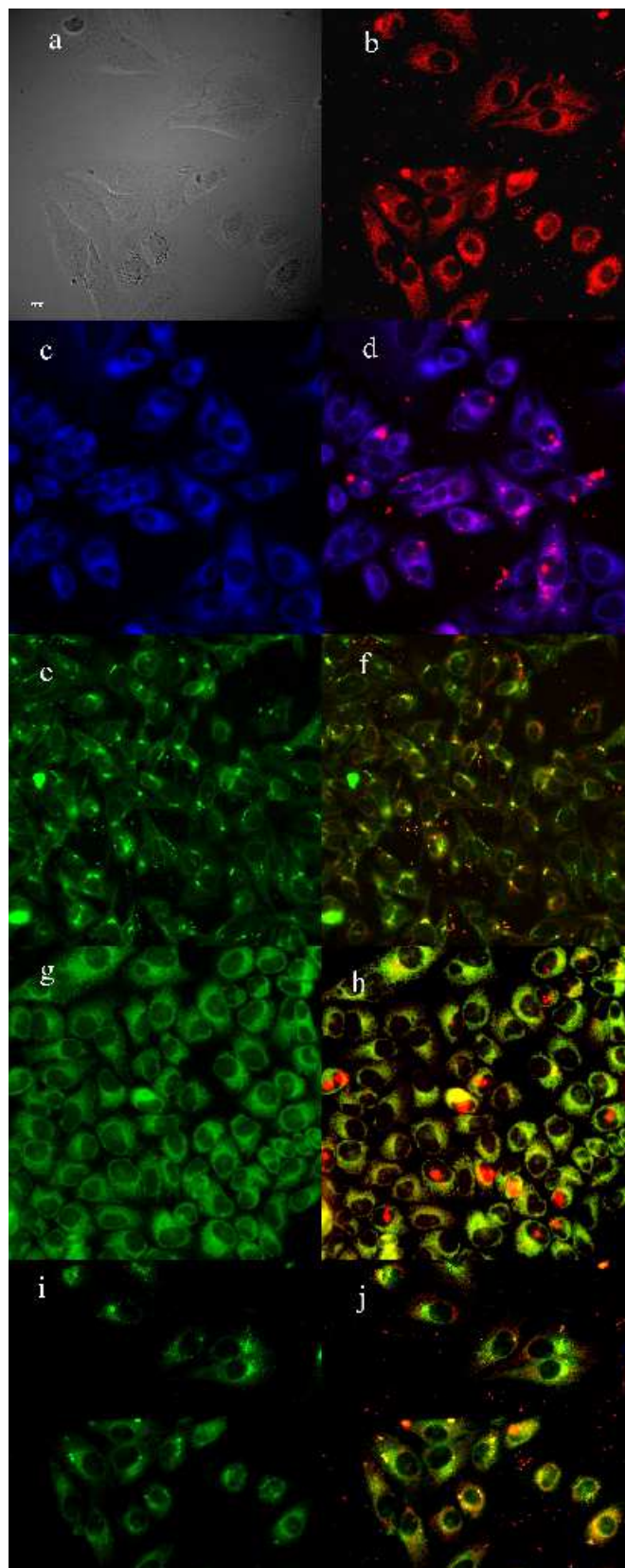




php\_13234\_f2.jpg

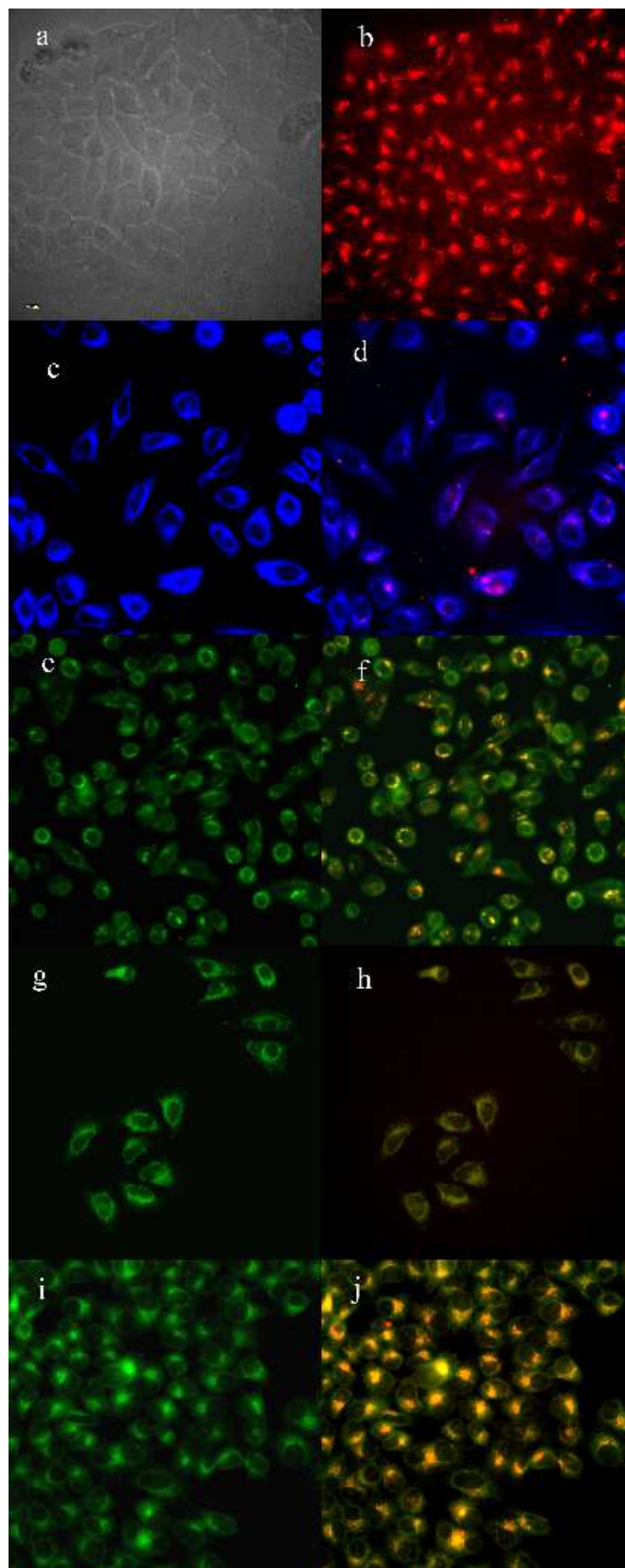


php\_13234\_f3.jpg



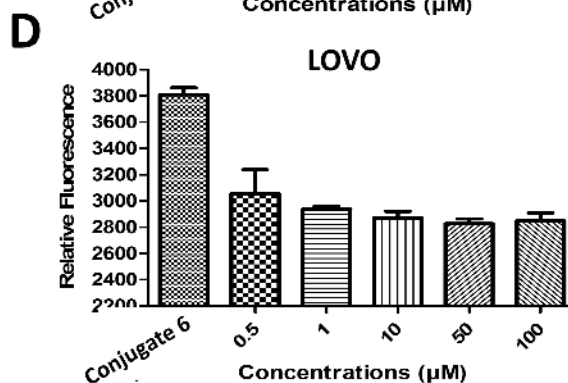
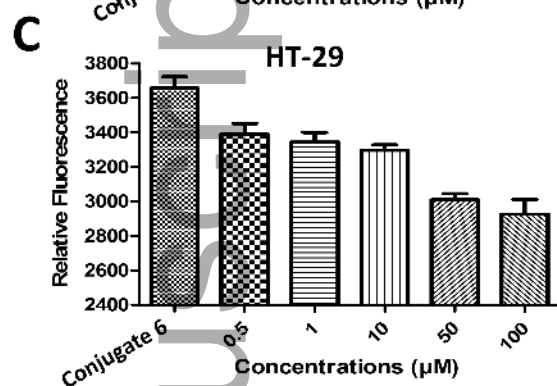
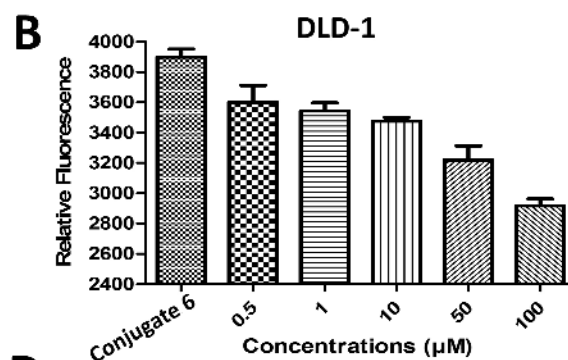
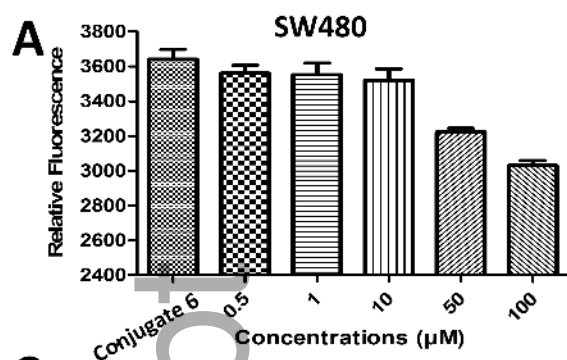
php\_13234\_f4.jpg



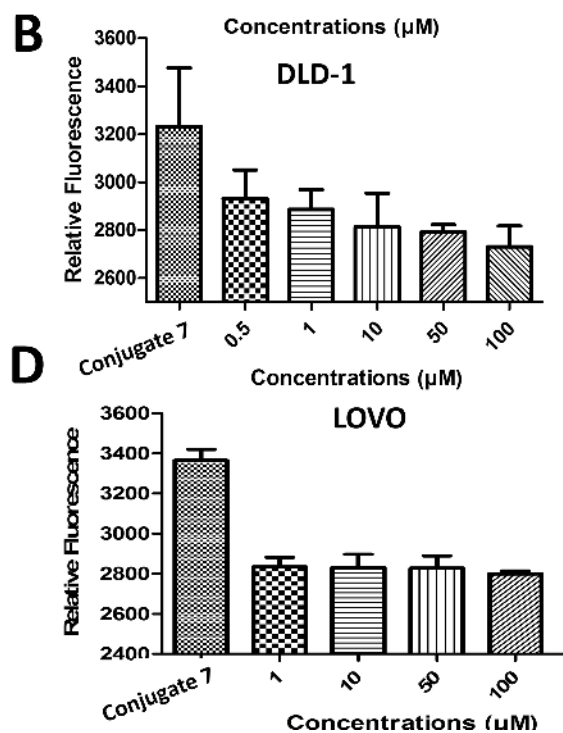
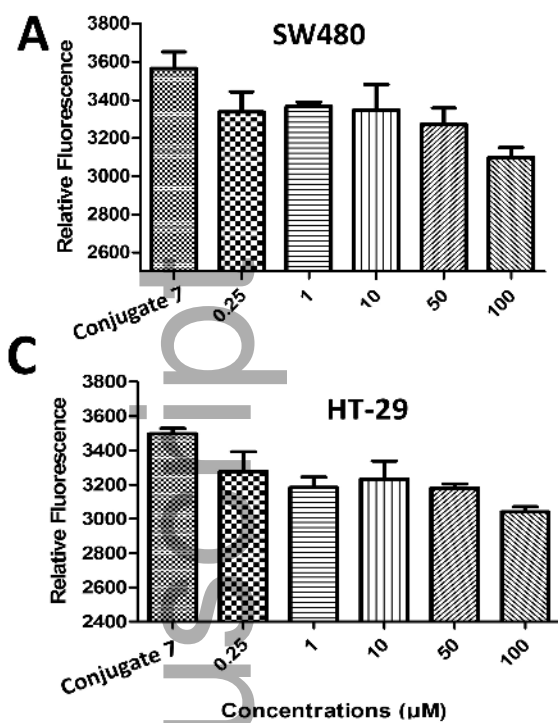


php\_13234\_f5.jpg

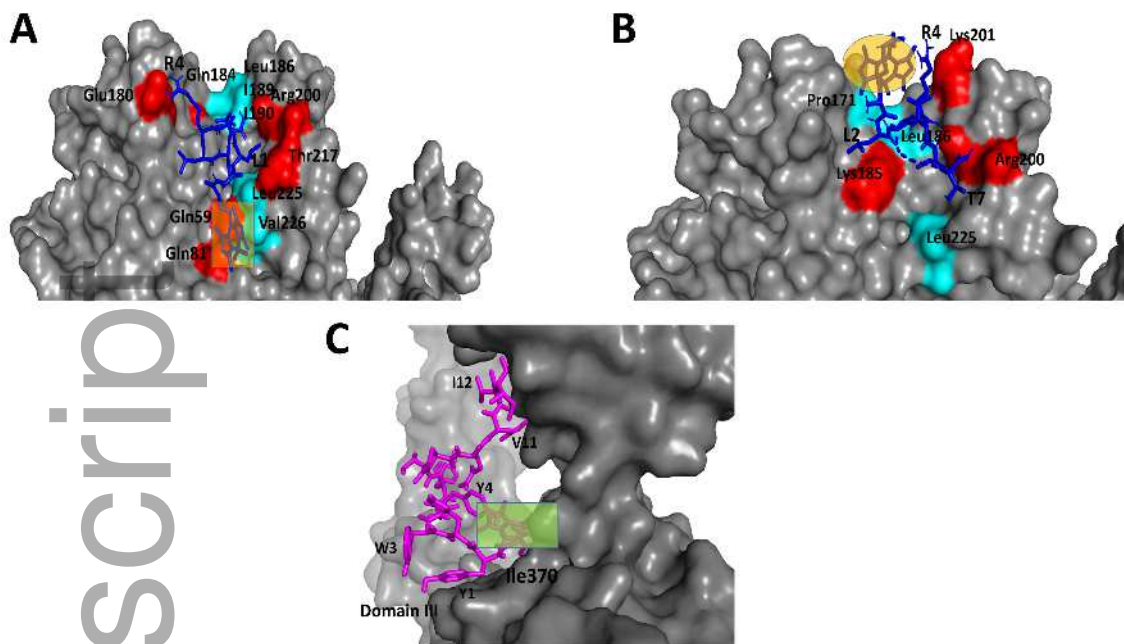




php\_13234\_f6.jpg



php\_13234\_f7.jpg



php\_13234\_f8.jpg